A REPORT ON THE RECENT CONFERENCE ON "SEMIMETALS AND NARROW GAP SEMICONDUCTORS"

G. Saunders

A REPORT ON THE RECENT CONFERENCE ON « SEMIMETALS AND NARROW GAP SEMICONDUCTORS »

G. A. SAUNDERS

Department of Applied Physics, the University of Durham, England

Résumé. — L'étude des matériaux de faible bande interdite a été poussée par leurs applications possibles, en particulier la réfrigération thermoélectrique et thermomagnétique, les dispositifs utilisant l'effet Hall ou la magnétorésistance, et enfin les détecteurs et les sources pour l'infrarouge.

Les derniers progrès dans ce domaine ont été exposés à la Conférence de l'Institut de Physique (Institute of Physics) sur « Les Semimétaux et les Semiconducteurs à faible bande interdite » (Semimetals and Narrow Gap Semiconductors) qui s'est tenue au Département de Physique Appliquée de l'Université de Durham (G.-B.) du 2 au 4 avril.

Abstract. — Study of materials with energy gaps close to zero has been spurred by possible applications including, among others, thermoelectric and thermomagnetic refrigeration, Hall and magnetoresistance devices and infrared sources and detectors. Recent progress in the field was surveyed at the Institute of Physics' conference on « Semimetals and Narrow Gap Semiconductors » held at the Department of Applied Physics, the University of Durham, 2nd-4th april, 1968. The present paper is a concision of the varied work reported at that conference ; only a small part is reviewed, and many interesting reports are not touched on.

I. **Sample Preparation.** — Applications are not limited to pure elements and compounds : solid solutions are also of use. For example, extensive studies of the bismuth-antimony alloys were instigated by their possible use in thermoelectric cooling at low temperatures. An important feature is the retention of high carrier mobilities and long carrier mean free paths on alloying : carrier densities remain low in the alloys, and the de Broglie wavelength of carriers at the Fermi surface is too long to resolve the local perturbations produced by isoelectronic impurities. In a review of the transport properties of the bismuth-antimony alloys, H. J. Goldsmid (Bath University) set the scene for repeated discussions during the conference of the necessity of achieving homogeneity and purity in low gap alloys and compounds. Crystal growth techniques, reviewed in detail by S. E. R. Hiscocks and D. T. J. Hurle (Royal Radar Establishment) assume prime importance ; in particular constitutional supercooling can lead to cellular segregation with consequent inhomogeneity and high dislocation densities. Very slow growth rates and steep temperature gradients are prerequisite in preventing microsegregation of components.

One notable advance in the growth of crystals with one or more volatile components is the technique of liquid encapsulation : crystals are pulled or Bridgman-grown from melts covered with an inert, glassy film while an ambient pressure in excess of the vapour pressure of the volatile component is maintained to suppress evaporation. This method (see Fig. 1) avoids a high outer container temperature and the many difficulties associated with pulling from an enclosed container at high temperature. Boric oxide B_2O_3 is a most effective encapsulant : it is inert, transparent, forms a glass which wets silica, is an effective solvent for metal oxides and is easily dissolved away from the crystal surface by hot water. Materials grown at R. R. E. by this method include among others PbTe, SnTe, GeTe, $Pb_xSn_{1-x}Te$, $Ge_xSn_{1-x}Te$, $Hg_{1-x}Cd_xTe$, Cd_3As_2, GaAs and Bi.

Both SnTe and PbTe have appreciable vapour pressures near their melting points. Recently Hiscocks and West [1] have grown $Pb_{1-x}Sn_xTe$ single crystals to closely controlled compositions from melts encapsulated with B_2O_3 by the Czochralsky technique. The onset of constitutional supercooling as a function of growth rate was investigated, and cell structure was found for pull rates above 10 mm/h. Crystals grown at 5 mm/h were apparently free of cell structure but, to allow a safety margin, growth rates between 1 and 3 mm/h were normally employed.

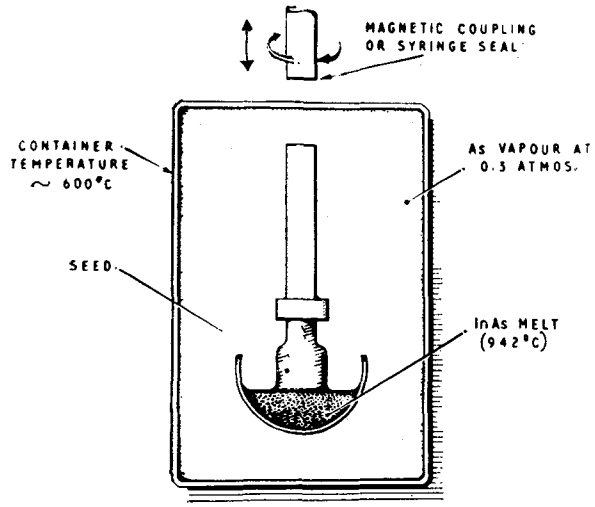

FIG. 1a. — The normal method of crystal pulling involves the enclosure of the crucible and seed assembly in a silica container maintained at high temperature to prevent condensation of volatile components.

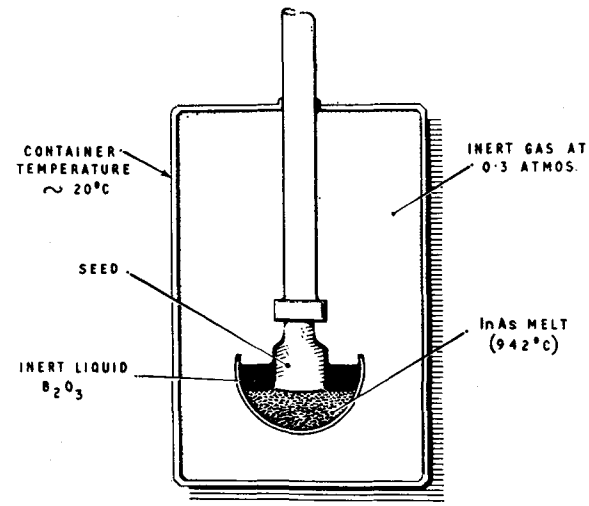

FIG. 1b. — The liquid encapsulation technique (published by kind permission of S. E. R. Hiscocks).

II. **Solid Solutions.** — Solid solution systems of particular interest comprise the PbTe-SnTe and PbSe-SnSe alloys with the rock salt crystal structure ; some recent work on crystal growth, annealing and diffusion and electrical properties of lead-tin chalcogenides at the Lincoln Laboratory was outlined by T. C. Harman [2, 3]. Other reports will be given at this present conference and a very brief summary is adequate here. As the tin content is increased, the energy gap decreases until it goes through zero for $Pb_{0.65}Sn_{0.35}Te$ and $Pb_{0.865}Sn_{0.135}Se$. The effective mass decreases with the energy gap. Here at hand are variable band gap materials available for fabrication of tunable long wavelength infrared lasers or detectors : the wavelength emitted from a semiconductor injection laser is close to that corresponding to the band gap energy, near zero for these alloys. During the conference Harman reported [4] that diode lasers have now been constructed giving an emitted wavelength of 28 μ from $Pb_{0.73}Sn_{0.27}Te$.

With PbTe-SnTe or PbSe-SnSe alloys infrared detection can be achieved at longer wavelengths than with the pure binary compounds themselves ; several workers reported extension of the long wavelength limit, including in their measurements response at 10.6 μ, the wavelength of the CO_2 laser. The relatively poor values of the figure of merit D* attained to date are possibly indicative of the early stage of development. These alloys show potential as infrared detectors in optical communications systems through the atmospheric window for which wideband, sensitive detectors are desirable.

Other alloy systems in which the interesting zero gap condition is obtainable include Bi-Sb, HgTe-CdTe and Hg_3Te_3-In_2Te_3. The relationship between the band structure and electrical properties of the Hg_3Te_3-In_2Te_3 alloys, studied extensively by D. A. Wright and his co-workers [5], was reported at the conference. HgTe itself is a semimetal. Addition of In_2Te_3 reduces the band overlap linearly with lattice parameter as far as 37.5 % molecular In_2Te_3. The zero gap alloy has a composition corresponding to 5 % molecular In_2Te_3. The electron effective mass is low ($< 0.04\ m_0$) and mobility rather high.

III. **The Band Structures and Transport Properties of the Group V Semimetals and the IV-VI Compounds.** — A high proportion of the papers presented at the conference were concerned with aspects of either band structure determinations or carrier transport properties. Reviews falling into this regime included those given by H. J. Goldsmid (Bi-Sb alloys), M. G. Priestley (de Haas-van Alphen effect), D. L. Greenaway (optical reflectivity techniques), G. A. Saunders (galvanomagnetic effects) and T. C. Harman (lead-tin chalcogenides).

Much of the work discussed related to the Group V elements As, Sb and Bi. These crystallize in a rhombohedral ($\bar{3}\ m$) crystal structure which can be obtained from the simple cubic structure (made from two inter-

penetrating fcc lattices) by a shear, applied along a cube diagonal so that the rhombohedral angle α is reduced (from 60° to 54°10′ for As, 57°6.5′ for Sb and 57°14.2′ for Bi), combined with an internal displacement of atoms along this body diagonal. This crystal structure is closely related to that of the IV-VI compounds and an outline of the band structures and transport properties of the Group V elements provides an interesting point of comparison for IV-VI compounds.

In the materials of distorted structure, band overlap leads to semimetallic behaviour [6]. States near the band edge in the sixth zone are lower in energy than those in the fifth zone : a small number of electrons spill over into the conduction band to leave an equal number of holes in the valence band ; the carrier density in each band is $3 \times 10^{17}/\text{cm}^3$ for bismuth [7], $4.2 \times 10^{19}/\text{cm}^3$ for antimony [8] and $2.1 \times 10^{20}/\text{cm}^3$ for arsenic [9, 10]. Characteristic carrier properties are small effective masses, high mobilities and long electron-lattice relaxation times ; quantum effects are relatively large ; the semimetals are particularly suitable vehicles for experimental band structure studies and for testing new aspects of electron theory. Much research has been carried out for bismuth. Detailed band structure calculations have now been completed for bismuth [11], antimony [12] and arsenic [13] using the pseudopotential approach. These accord with experimental data : the essential features of the Fermi surfaces are now mapped out and turn out to be rather complicated, as might be expected from the distorted crystal structure. All these semimetals have similar electron surfaces, namely sets of six warped half ellipsoids, which coalesce into three warped whole surfaces, centred about energy minima at the centres of the six irregular hexagon faces of the Brillouin zone (Fig. 2). These minima lie in the three reflection planes. Each electron ellipsoid has one principal axis coincident with an axis of two-fold symmetry — there are three of these, each obtainable from the others by a rotation of ± 120° about the trigonal axis — while the other ellipsoid principal axes lie in the mirror plane.

The configuration is illustrated in figure 3. The tilt angles ψ_e are collected in Table 1. In the *A*7 arsenic structure rotations by identical amounts in the mirror plane away from the trigonal axis towards the directions ΓX or ΓL are not equivalent [14]. To avoid ambiguity, the sense of the tilt angles must be defined

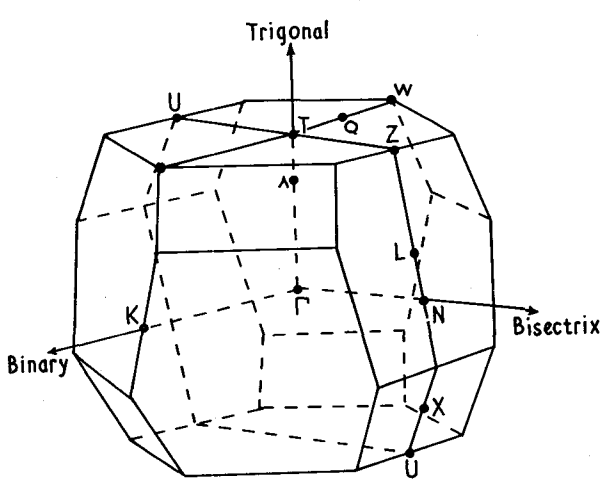

FIG. 2. — The Brillouin zone of the Group V semimetals, showing those symmetry points, in standard notation, prerequisite for the positioning of the Fermi surface extrema.

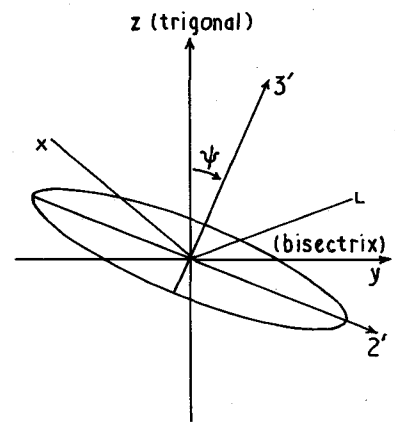

FIG. 3. — Cross section of an ellipsoid surface in the trigonal-bisectrix plane to illustrate the orientation relative to the crystal axes of the axes (1′, 2′, 3′) of the principal ellipsoid. The binary axis of the crystal coincides with the 1′ ellipsoid axis. The angle ψ refers to rotation away from the trigonal axis in the quadrant containing ΓT, ΓL and ΓN.

TABLE I

The tilt angles of the Fermi surface pockets in the Group V semimetals.

		Electron pockets		Hole pockets	
	Reference	Number	Tilt Angle	Number	Tilt Angle
Bi	25	3	6°	1	0°
Sb	20	3	6.5°	6	31°
As	13, 9, 10	3	8° ± 2°	6 pockets connected by necks	40° ± 2°

The tilt angle refers to the angle between the trigonal axis and the shorter of the ellipsoid principal axes in the mirror plane. The rotation is taken away from the trigonal axis toward ΓL in the quadrant containing ΓT, ΓL and ΓN (for As and Sb).

through specification of the direction employed for this rotation. Experimentally this is made easier from back-reflection Laue photographs : the direction ΓL gives rise to a prominent pseudo-trigonal point and ΓX to a pseudo-fourfold point.

The hole surfaces differ considerably from one semimetal to another ; in bismuth there is one ellipsoid of rotation about the trigonal axis, while in antimony and arsenic there are six highly tilted pockets, see table I, those in arsenic being connected by six small « necks » to form the « crown » shown in figure 4.

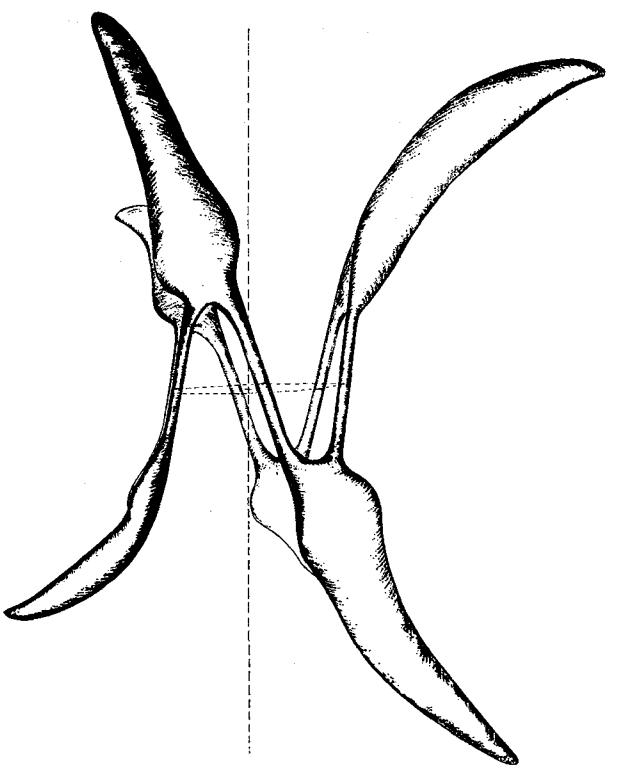

FIG. 4. — The hole Fermi surface in arsenic predicted by the pseudopotential band structure calculation of Lin and Falicov [13].

As the Fermi surface volume expands through the sequence bismuth, antimony and arsenic, the carrier effective masses increase. Some of the considerable data in the literature are collected in table II.

One intent of Fermi surface studies is to sharpen our understanding of transport properties. Fundamental details of the band and mobility parameters can now be deduced from measurements of the galvanomagnetic effects. For the $\bar{3}m$ structure there are twelve independent components of the magnetoresistivity tensor to second order in magnetic field [15].

TABLE II

Effective mass tensor components along the principal ellipsoid axes in the group V semimetals.

	Refe-	Electrons			Holes		
	rences	m_1	m_2	m_3	m_1	m_2	m_3
Bi ([a])	26	0.14	0.009	0.11	0.067	0.067	0.23
Sb ([b])	27	0.093	1.14	0.088	0.068	0.92	0.050
As	9	0.163	2.11	0.105			

([a]) The data for bismuth depends very much upon the sample and values in the literature vary widely.
([b]) Carrier signs assumed in reference 27 are inverted.

Abeles and Meiboom [16] first showed that the galvanomagnetic effect data in bismuth can be interpreted on the basis of the Fermi surface model just described. The method is incapable of providing an independent determination of the number of ellipsoids. A valuable feature is that galvanomagnetic effects do allow direct experimental discrimination between the carriers. Until recently little experimental evidence was available to assign the electrons and holes to the two sets of pockets found for both antimony and arsenic. Indeed for antimony the carriers in the highly tilted pockets were conventionally, although incorrectly, alluded to as electrons. This led to much confusion. Measurements of the magnetoresistivity tensor in antimony [8], tin-doped antimony [17] and arsenic [10] have sited the holes in each case in the most canted pockets. This is in agreement with the predictions [12, 13] of the pseudopotential band structure calculations. Comparison between the carrier mobility ratios (collected in table III) in these semimetals and the effective mass ratios indicates that the variation between components of the relaxation time tensor does not exceed two.

TABLE III

Carrier mobilities in the ellipsoid coordinate system for arsenic at 305 °K and antimony at 273 °K, assuming ellipsoidal energy surfaces.

	Electrons			Holes		
	μ_1	μ_2	μ_3	γ_1	γ_2	γ_3
Sb[8]	2 740	110	1 950	3 630	180	3 220
As[10]	460	40	550	1 210	50	680

Units : $cm^2\ v^{-1}\ s^{-1}$.

In arsenic high mobility holes [13] in the connecting necks may play a role in the transport properties [10]. One interesting question arises in the antimony-tin alloys containing carrier densities of the same order

as in arsenic : are the hole pockets expanded into a crown-like surface ? Measurement of the magnetoresistivity tensor do provide evidence for the existence of light holes in alloys containing between 2 at. % and 8 at. % tin [18]. The density of this second set of carriers is about 1 % of that of the majority holes. Figure 5 is a schematic of the possible band structure. The present experiments do not allow distinction between the elementary model and one in which the Fermi surface is multiply-connected. Here too the difficulties of preparation of homogeneous alloys come into play ; results must be treated cautiously. However, recently Hauser and Testardi [19] have observed tunneling structure in pure antimony which evidences this second set of holes.

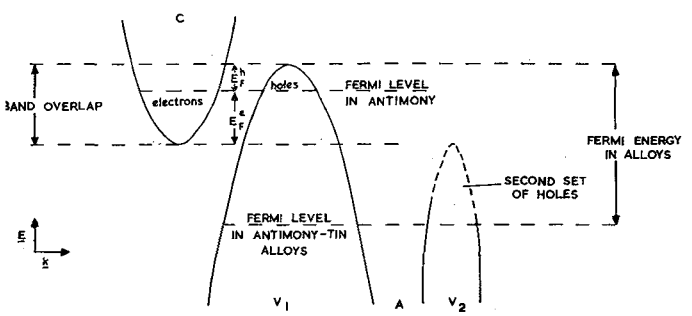

FIG. 5. — Schematic diagram of the electron (C) and hole (V_1 and V_2) bands in antimony and antimony-tin alloys. Galvanomagnetic experiments cannot readily distinguish between this model and that in which V_1 and V_2 are joined at A : in the latter case with the Fermi level below the junction, a multiply-connected surface would result.

For the pure elements antimony and bismuth at least, the carrier transport properties can be resolved quite well using the multivalley model with ellipsoidal energy surfaces and parabolic bands. But there are discrepancies. For antimony the magnetoconductivity tensor analysis gives 24° for the angle ψ_h of the hole pockets and a carrier density in each band of $4 \times 10^{19}/\text{cm}^3$ in contrast to values of $\psi_h = 31°$ and $N = 5.5 \times 10^{19}/\text{cm}^3$ obtained from the de Haas-van Alphen effect data [20]. The Fermi surface is not ellipsoidal [12, 14]. A characteristic of narrow gap semiconductors and materials having band edges close together is a non-parabolic $E - k$ relationship, resulting from mutual interaction between the bands through the $k.p$ interaction. Two models are now in favour : those of Lax (ellipsoidal, non-parabolic) and Cohen (non-ellipsoidal, non-parabolic). These models have been examined extensively for the conduction band in bismuth but it is difficult to distinguish between them : they provide similar conditions over much of the Fermi surface and differ essentially along the less accessible heavy mass direction [11]. A sensitive test of the models is to look for changes, predicted only by the Cohen model, in the Fermi surface anisotropy with doping or application of hydrostatic pressure.

Cohen's model has been extended to the IV-VI compounds, such as PbS, PbSe, PbTe and SnTe, which have a closely related crystal structure to the group V semimetals. Cohen gives the dispersion relation for carriers at the symmetry points in the Brillouin zone where band extrema are sited. During the conference it became clear that the transport properties in the near zero gap IV-VI compounds, as well as the group V semimetals, can only be unambiguously interpreted using the non-ellipsoidal, non-parabolic band model (see Allgaier [21] and Rogers [22] for references in this field).

IV. **The magnetophonon effect.** — The review paper presented by R. A. Stradling (Oxford University) on the magnetophonon effect aroused great interest. Gurevich and Firsov [23] first predicted this new oscillatory phenomenon in the transverse magnetoresistance in semiconductors in a strong magnetic field defined by the condition

$$\Omega\tau = eH\tau/m^* c = \mu H/c \gg 1$$

where Ω is the cyclotron frequency, τ is the electronic relaxation time and μ is the carrier mobility. Figure 6

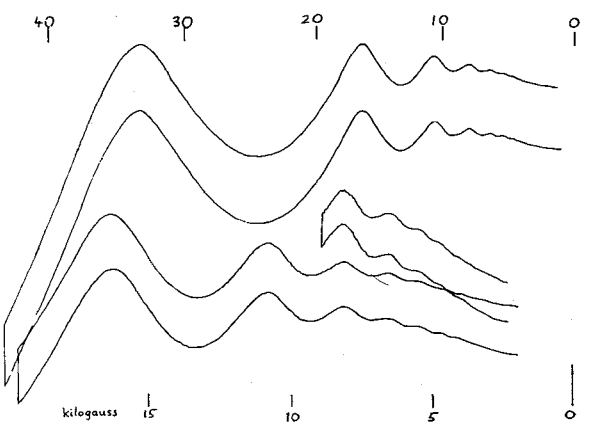

FIG. 6. — Magnetophonon oscillations in n-InSb at 100 °K (published by kind permission of R. A. Stradling).

illustrates the oscillations observed in n-type InSb by R. A. Stradling. Physical insight into the effect can be gained on the model sketched in figure 7. When the energy $\hbar\omega_L$ of the longitudinal optical phonons is equal to the energy separation between the Landau levels $N\hbar\Omega$, the probability of scattering

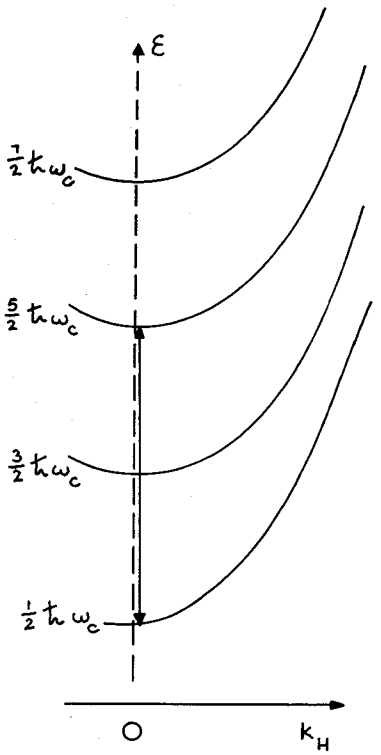

FIG. 7. — Magnetophonon effect : the inelastic interaction between electrons in the Landau levels and the longitudinal optical mode phonons can take place whenever

$$\omega_L = N\Omega = NeH/m^* c$$

(published by kind permission of R. A. Stradling).

of electrons with these optical phonons increases markedly and the resistivity component ρ_{xx} rises (the magnetic field H is aligned parallel to the z-axis). Thus the condition for resonant absorption is

$$\hbar\omega_L = N\hbar\Omega$$

and this inelastic interaction gives rise to a periodic oscillation in the magnetoresistance of a form

$$\Delta(1/H) = e/m^* \omega_L c$$

different from the de Haas-Shubnikov effect. Conditions for observation of the effect include a high carrier mobility and sufficient optical mode phonons. The latter condition necessitates a moderately high temperature : the optimum temperature for InSb is 104 °K [24]. Here is a powerful method for estimating either the longitudinal optical phonon frequency or the carrier effective mass without recourse to the expensive hardware of cyclotron resonance. Both longitudinal and transverse magnetoresistance effects of this nature have been observed in several materials, but so far not in IV-VI compounds.

References

[1] HISCOCKS (S. E. R.) and WEST (P. D.), *J. Materials Science*, 1968, **3**, 76.
[2] DIMMOCK (J. O.), MELNGAILIS (I.) and STRAUSS (A. J.), *Phys. Rev. Letters*, 1966, **16**, 1193.
[3] CALAWA (A. R.), HARMAN (T. C.), FINN (M.) and YOUTZ (P.), Trans. Met. Soc., AIME, March, 1968.
[4] BUTLER (J. F.), CALAWA (A. R.) and HARMAN (T. C.), *Applied Phys. Letters*, 1966, **9**, 427.
[5] WRIGHT (D. A.), *Brit. J. Appl. Phys.*, 1965, **16**, 939.
[6] COHEN (M. H.), FALICOV (L. M.) and GOLIN (S.), *IBM J. Res. and Dev.*, 1964, **8**, 215.
[7] BHARGAVA (R. N.), *Phys. Rev.*, 1967, **156**, 785.
[8] ÖKTÜ (O.) and SAUNDERS (G. A.), *Proc. Phys. Soc.*, 1967, **91**, 156.
[9] PRIESTLEY (M. G.), WINDMILLER (L. R.), KETTERSON (J. B.) and ECKSTEIN (Y.), *Phys. Rev.*, 1967, **154**, 671.
[10] JEAVONS (A. P.) and SAUNDERS (G. A.), *Phys. Letters*, 1968, **27A**, 19.
[11] GOLIN (S.), *Phys. Rev.*, 1968, **166**, 643.
[12] FALICOV (L. M.) and LIN (P. J.), *Phys. Rev.*, 1966, **141**, 562.
[13] LIN (P. J.) and FALICOV (L. M.), *Phys. Rev.*, 1966, **142**, 441.
[14] WINDMILLER (L. R.), *Phys. Rev.*, 1966, **149**, 472.
[15] JURETSCHKE (H. J.), *Acta Cryst.*, 1955, 8, **716**.
[16] ABELES (B.) and MEIBOOM (S.), *Phys. Rev.*, 1956, **101**, 544.
[17] ÖKTÜ (Ö.) and SAUNDERS (G. A.), *Physics Letters*, 1967, **25A**, 266.
[18] SAUNDERS (G. A.) and ÖKTÜ (Ö.), *Physics Letters*, 1967, **27A**, 604.
[19] HAUSER (J. J.) and TESTARDI (L. R.), *Phys. Rev. Letters*, 1968, **20**, 12.
[20] WINDMILLER (L. R.) and PRIESTLEY (M. G.), *Sold State Commun*, 1965, **3**, 199.
[21] ALLGAIER (R. S.), *Phys. Rev.*, 1966, **152**, 808.
[22] ROGERS (L. M.), *Brit. J. Appl. Phys.*, 1967, **18**, 1227.
[23] GUREVICH (V. L.) and FIRSOV (Yu. A.), *Sov. Phys. JETP*, 1961, **13**, 137.
[24] FIRSOV (Yu. A.), GUREVICH (V. L.), PARFENIEV (R. V.) and SHALYT (S. S.), *Phys. Rev. Letters*, 1964, **12**, 660.
[25] ZITTER (R. N.), *Phys. Rev.*, 1962, **127**, 1471.
[26] KAO (Y.-H.), *Phys. Rev.*, 1963, **129**, 1122.
[27] DATARS (W. R.) and VANDERKOOY (J.), *IBM J. Res. Dev.*, 1964, **8**, 247.